ECS Journal of Solid State
Science and Technology

Study of Amperometric Response of Guaiacol Biosensor Using Multiwalled Carbon Nanotubes with Laccase Immobilized

ECS Journal of Solid State Science and Technology, 2020 **9** 115009

Study of Amperometric Response of Guaiacol Biosensor Using Multiwalled Carbon Nanotubes with Laccase Immobilized

E. G. Uc-Cayetano,[1,z] I. E. Villanueva-Mena,[1] M. A. Estrella-Gutiérrez,[1] L. C. Ordóñez,[2] O. E. Aké-Uh,[1] and M. N. Sánchez-González[1]

[1] *Universidad Autónoma de Yucatán, Facultad de Ingeniería Química, Chuburná de Hidalgo Inn, Mérida, Yucatán, México*
[2] *Centro de Investigación Científica de Yucatán, Unidad de Energía Renovable, C.P. 97302 Sierra Papacal, Yucatán, México*

Multiwalled Carbon Nanotubes (MWCNTs) were used as a support of amperometric enzymatic biosensors of guaiacol. The structural quality of MWCNTs was determined for Raman Spectra and DRX analysis. MWCNTs were decorated with iron oxide nanoparticles (36 w/w%), which were observed by FE-SEM, and were confirmed by with EDX, and TGA analysis. Laccase enzyme *(aspergillus sp.)* was immobilized on the surface of MWCNTs (oxidized and decorated with iron oxide nanoparticles) confirmed by XPS analysis and used to amperometric detection of guaiacol. The material obtained was deposited on the active surface of glassy carbon electrode (GCE) and was carried out using a typical three-electrode system with saturated calomel electrode as a reference and a graphite rod as a counter-electrode. The results confirm the potential use of bioelectrode Lac/MWCNTs/GCE and Lac/Fe_3O_4/MWCNTs/GCE for the guaiacol detection in low concentrations. Amperometric sensitivities and detection limits of Lac/Fe_3O_4/MWCNTs/GCE bioelectrode (110.186 μA mMcm^{-2} and 34.301 nM for reduction current respectively) showed better results than Lac/MWCNTs/GCE bioelectrode in a linear range 0–0.066 μM of guaiacol.
 [DOI: 10.1149/2162-8777/aba8da]

Manuscript received July 1, 2020. Published July 30, 2020. *This paper is part of the JSS Focus Issue on Solid-State Materials and Devices for Biological and Medical Applications.*

Polyphenols are found naturally in plants, condiments and spices. They have an important role in human health and nutrition, because they contribute to the taste of wine, tea, olive oil, and have antioxidant and anti-inflammatory capacity, which provides the body protection against some diseases.[1–3] Today, spectrophotometry, capillary electrophoresis, gas chromatography-mass spectroscopy (GC-MS), and HPLC are quite powerful analytical techniques for the determination of polyphenols from various samples. However, these techniques require a lot of time, expensive equipment, various pretreatments and solvents that are not always environmentally friendly.[4,5]

According to IUPAC, a biosensor is a device that uses specific biochemical reactions mediated by enzymes or other biological elements to detect chemical compounds usually by electrical, thermal or optical signals. These mentioned biological elements come into direct contact with the analyte, generating a particular change that can be measured in the transductor. If the recognition element is an enzyme, it is known as an enzymatic biosensor. Most of the enzymatic biosensors developed so far are electrochemical in nature since the analyte is recognized by immobilized enzymes in working electrodes and its electrocatalytic activity can cause electronic transfer, producing either current or voltage. This kind of biosensors are preferable due to its low cost, relatively fast response times, ease of use and small size.[6,7]

Recently, several polyphenol biosensors have been developed that use redox enzymes such as tyrosinase, peroxidase, laccase, among others. Laccase biosensors being the simplest to build because this enzyme does not require hydrogen peroxide (H_2O_2) as a co-substrate or any other cofactor to modify its catalytic action.[7] Laccase (benzenediol:oxygen oxidoreductases, EC 1.10.3.2) is a dimeric or tetrameric glycoprotein, which contains four copper atoms per monomer distributed at three redox sites. This enzymes catalyzes the oxidation of various inorganic and aromatic compounds (like a phenols) and the reduction of molecular oxygen to water.[5,8] Laccases can be applied to certain processes that improve or modify the color appearance of food or beverages, so some of their applications consist in the elimination of undesirable polyphenols, responsible for blackening and the formation and development of turbidity in juices fruit, beer and wine. They have also been applied to different processes, mainly the development of biosensors, fuel cells and the oxidation of organic pollutants.[8]

Recently, the use of nanomaterials (specially of carbon and metals) has led to an improvement in the analytical performance of enzyme biosensors. Since their discovery in the nineties, carbon nanotubes (CNTs) have proven to be an extremely versatile material due to their incredible physical, physicochemical and electrochemical properties, of which, their excellent thermal, electrical and mechanical properties, they make them a good candidate for applications in the sensing and detection of moisture, gases and various analytes and biomolecules.[9,10] The sensing of biomolecules, such as enzymes, proteins, biomarkers, cells, microorganisms and even DNA using biosensors based on single and multiple wall carbon nanotubes have been widely reported in the literature.[11–14]

Enzymatic electrochemical biosensors have been fully used in health care, environmental monitoring and food safety, being one of the most common glucose biosensors. The use of these biosensors constitutes an economic and simple analytical method with remarkable detection sensitivity, reproducibility and ease of miniaturization. The electrodes that include carbon nanotubes in their manufacture, exhibit a low detection limit and a rapid response due to the improvement of the signal provided by the high surface area, low overvoltage and rapid electrode kinetics and have presented numerous advantages in the analysis of various chemical products of food, clinical or environmental interest.[6,15]

Although there are advances in this area, it is possible to improve the electrochemical response of electrodes modified with carbon nanotubes, physicochemical modified being one of the most promising ways to improve this response. Twice of the most used superficial modification of carbon nanotubes techniques is plasma and acid treatments.[15] It has been found that, the deposition of metallic nanoparticles on the surface of carbon nanotubes helps to decrease the response time of the biosensor, improve electron transfer and increase its electrocatalytic activity.[16]

Some authors have reported the use of enzymatic biosensors of immobilized laccase on carbon nanotubes using Au, Ag, Ni and Zn nanoparticles,[4,7,17] however, this work explores the incorporation of iron oxide nanoparticles because it has a small size (with respect to CNTs) and good electrical and magnetic properties in addition to its shape is also conducive to enzyme immobilization, which could result in an improvement in the performance of the biosensor. Other works have already reported the decoration of the walls of CNTs

[z] E-mail: erbin.uc@correo.uady.mx

with iron oxides in enzymatic biosensors for the detection of glucose,[18] however, the use of this class of nanoparticles in this type of applications is relatively low. Therefore, the goal of this work is the amperometric detection of polyphenols (specially guaiacol) using enzymatic biosensors with immobilized laccase in CNTs oxidized and decorated with iron oxides nanoparticles.

Experimental

Materials.—Commercial MWCNTs (Cheap Tubes Inc., Brattleboro, USA) with purity >95 wt.% and <1.5% of ash, outer and inner diameter of 50–80 and 5–10 nm, respectively were used. They have length ranging from 10–20 μm and electrical conductivity >100 S cm^{-1}. The measured BET surface area was 90 m^2 g^{-1} (Fig. 1) and the average Raman ratio for I_G/I_D intensity is 1.57 (Fig. 3).

For oxidation process, were used nitric acid (70% v/v) and sulfuric acid (98.6% v/v), both of J.T. Baker; iron (III) chloride hexahydrate (99% v/v); triethylene glycol (TREG, 99% v/v) and anhydrous sodium acetate (99% w/w) used for the nanoparticle decoration were acquired from Sigma-Aldrich. In addition, in order to prepare acetate buffer solution (ABS) with acetic acid and anhydrous sodium acetate was used.

Laccase enzyme expressed in *Aspergillus sp.* (⩾1000 units g^{-1}); N-(3-Dimethylaminopropyl)-N′-ethylcarbodiimide hydrochloride (EDAC) and N-Hydroxysuccinimide (NHS) were used for the immobilization process acquired from Sigma-Aldrich. Guaiacol ⩾ 98.0% acquired from Sigma-Aldrich was used as substrate in the electrolyte solution.

Oxidation, decoration and immobilization of laccase onto carbon nanotubes.—The as-received MWCNTs were oxidized with a mixture 8.0 M of HNO_3 and H_2SO_4 which has been proven an efficient generation of OH, CO and COOH functional groups.[19] This procedure consists in the dispersion of 0.3 g of MWCNTs in 70 ml of the mixture of these acids and stirring for 15 min at 60 °C, followed by 2 h of dispersion in an ultrasonic bath. Finally the MWCNTs were then washed with distilled water, filtered and dried at 100 °C for 12 h.

For the decoration of MWCNT with iron oxide nanoparticles, the method used[20] consisted of the ultrasonic dispersion of 100 mg of oxidized MWCNT in 50 ml of TREG for 1 h. After dispersion, 200 mg of $FeCl_3$*$6H_2O$ and 3.6 g of anhydrous sodium acetate were added to the solution. The resultant mixture was brought to reflux at 200 °C for 30 min, for later were centrifuged with acetone, washed and filtered with distilled water and finally dried at 100 °C for 12 h.

Laccase was immobilized over the surface of MWCNTs through amide/imide bonds formation by the reaction among carboxylic functional groups of the oxidized and decorated MWCNTs and amines groups of laccases, inspired in Ref. 21 For this, 10 mg of MWCNTs were dispersed using an ultrasonic bath in 10 ml of distilled water for 1 h, them in mechanical agitation, add 20 mg of EDAC followed by 30 mg of NHS under a nitrogen atmosphere. Upon dissolution of EDAC and NHS, 50 μl of laccase were added maintaining the agitation for 24 h. The MWCNTs with immobilized laccase were filtered, washed with distilled water and stored at 3 °C. The enzyme immobilization it was done in both oxidized only and oxidized and decorated MWCNTs (See Fig. 1).

Physicochemical and electrochemical characterization.—MWCNTs were characterized by Nitrogen adsorption–desorption isotherms at 77 K using a Micromeritics TriStar 3000 equipment. Morphology of only oxidized and decorated MWCNTs were observed by scanning electron microscopy (SEM) coupled with an energy dispersive X-ray (EDX) analyzer in a Jeol SEM 6360LB; Raman spectroscopy under similar conditions to the as-received MWCNTs, disperse 10 mg in 10 ml of acetone and deposited in a glass sample holder for us characterization. X-ray powder diffraction (XRD) was carried out at 40 kV, 20 mA, with a step time of 10 s and step angles of 0.02° in a Siemens D5000 diffractometer; the thermogravimetric analysis (TGA) was carried out in a TA Instruments analyzer at a heating rate of 10 °C min^{-1} under synthetic air flow of 20 ml min^{-1}. X-ray photoelectron spectroscopy (XPS) was performed with a Thermo K-Alpha spectrometer using a monochromatic Al X-ray source (1486.6 eV) and spot size of 400 μm.

Electrochemical analysis was performed at room temperature using an Autolab PG-STAT 302 potentiostat-galvanostat. Measurements

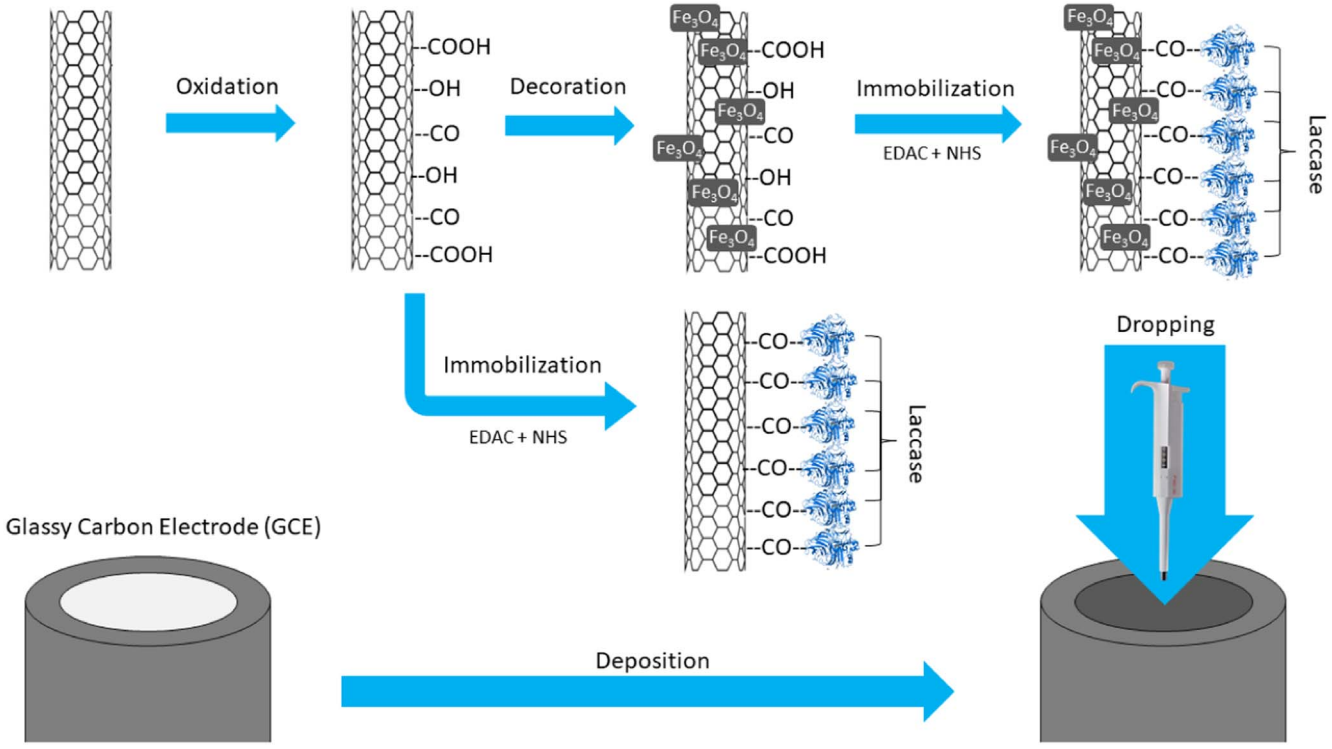

Figure 1. Schematic representation of the process performed in the MWCNT.

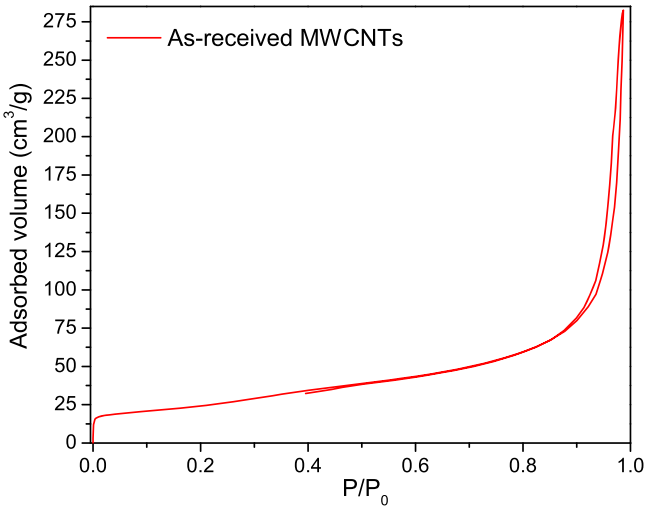

Figure 2. N_2 adsorption–desorption isotherms for as-received MWCNTs.

were carried out using a conventional three-electrode cell using a saturated calomel electrode (SCE, $Hg/Hg_2Cl_2/KCl$) as reference, a graphite rod as an auxiliary-electrode, and a glassy carbon electrode disk (GCE) with 3 mm diameter as a working electrode. The working electrodes were prepared depositing 10 μl of the solution with MWCNTs on the GCE disk by using a micropipette (Fig. 1). A scan rate of 50 and 25 mV s^{-1} was chosen for cyclic voltammetry (CV). The CV cycles showed reproducibility from the second cycle, and thus the third cycle was chosen as representative for CV. For selected sensing experiments, 1.0 M ABS (pH = 5.1) was used as electrolyte and different guaiacol concentrations was gradually added to the solution. Each experiment was repeated four times using different working electrodes and representative analytical curves are shown.

Results and Discussion

Physicochemical characterization.—Figure 2 shows the N_2 adsorption–desorption isotherms for complete range of partial pressure of as-received MWCNTs. These isotherms can be identified as "Type IV" according to the IUPAC classification,[22] corresponding to mesoporous materials with hysteresis loops occurring around 0.80\P/P_0\1. The BET specific area (S_{BET}) was 90.095 m^2 g^{-1} determined using the Brunauer, Emmett, and Teller equation[23] in the interval P/P_0 = 0.05–0.30.

The SEM micrographs of the MWCNT as-received and after the oxidation and decoration process can observed in Fig. 3. The dimensions of as-received MWCNTs are reasonably agree with those provided by the supplier, which is described in section Materials.

For as-received MWCNTs (Fig. 3a) the agglomeration of the material, traces of amorphous carbon and metal impurities are observed. The length and diameter of MWCNTs reported by the supplier are consistent. In Fig. 3b can observed the morphology of oxidized MWCNTs, which is similar to what was observed in Fig. 3a, with a little bigger dispersion. The acidic oxidation performed, slightly increases the density and extent of structural defects on the surface of the MCNT.[19] The presence of new functional groups in the external walls of the MWCNT was determined by changes in atomic and weight percentages of carbon and oxygen, which were obtained by EDX. Table I shows the percentage of carbon decreases and the percentage of oxygen increases after the oxidation process, due to the formed external bonds.

Figure 3c can observed MWCNTs decorated with iron oxide nanoparticles attached to the outer walls are seen in. The negatively charged functional groups on the surface of the oxidized nanotubes provide active sites for physical interactions with metal ions. In previous work we reported that the diameter of iron oxide nanoparticles were 1–10 nm.[20] The main elements present in the decorated samples (see Table I), reported in weight percentage are carbon (62.66%), oxygen (21.49%) and iron (21.49%).

Figure 4 shows representative Raman spectra of as-received, oxidized and decorated MWCNTs with iron oxide nanoparticles. Bands D and G were observed in the three different spectra. G band located around 1580–1600 cm^{-1} is a first-order Raman mode and corresponds to vibrations of sp^2 carbon atoms. The D band is originated from a second-order scattering process (around 1280–1350 cm^{-1}), which provides information about the presence of defects, vacancies and the finite size of the network what represents his loss of translational symmetry.[21] The intensity ratio between the G and D bands (I_G/I_D) can be used to characterize the structural ordering of the MWCNTs.[20–23]

For as-received MWCNTs Raman I_G/I_D intensity ratio is 1.57, while for oxidized MWCNTs, I_G/I_D = 1.528 and for decorated samples, I_G/I_D = 3.17. The increment in the value of I_G/I_D are a clear indication that the structural ordering is significantly less in the MWCNTs, for example with the decoration of iron oxide nanoparticles in the MWCNTs walls. In this case, the oxidation process generates more surface defects and, in consequence, new functional

Table I. EDX analysis of MWCNTs.

Element	Weight%	Atomic%
As-received MWCNTs		
C	97.32	97.97
O	2.68	2.03
Oxidized MWCNTs		
C	97.18	97.86
O	2.82	2.14
Decorated MWCNTs		
C	62.66	76.23
O	21.49	19.63
Fe	15.84	4.15

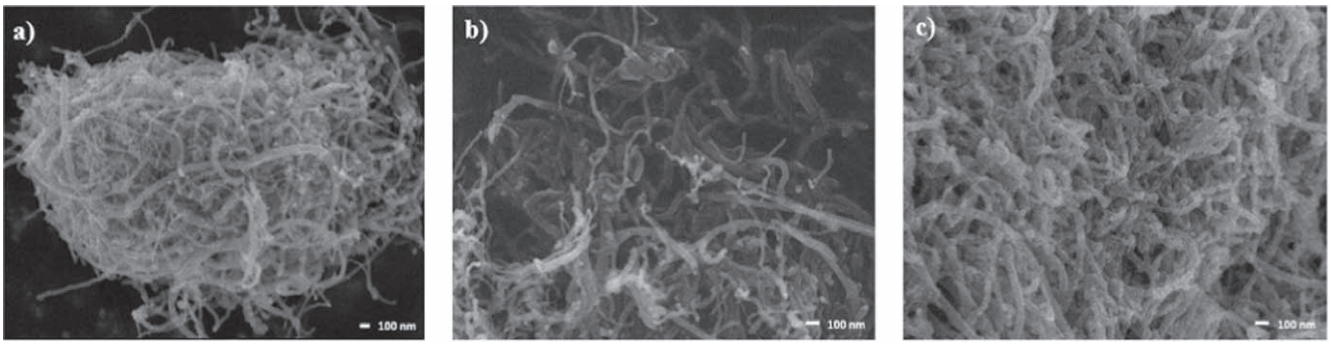

Figure 3. FE-SEM images of (a) As-received MWCNTs, (b) Oxidized MWCNTs and (c) Decorated MWCNTs with iron oxide nanoparticles.

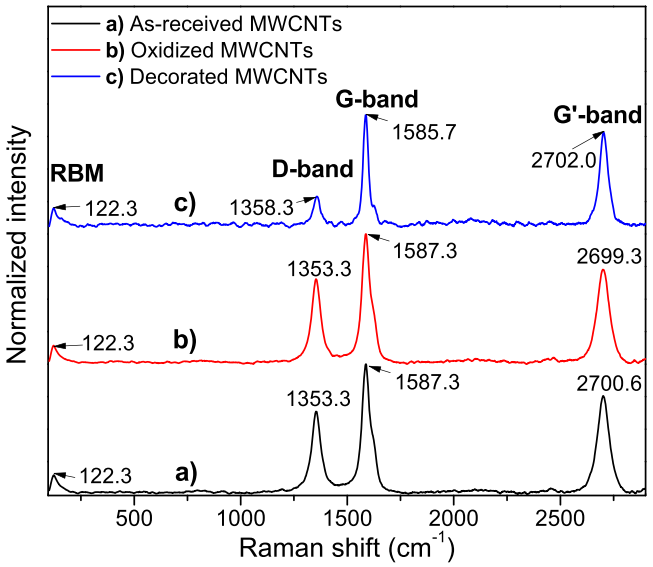

Figure 4. Raman spectra of (a) As-received MWCNTs (black line), (b) Oxidized MWCNTs (red line) and (c) Decorated MWCNTs with iron oxide nanoparticles (blue line).

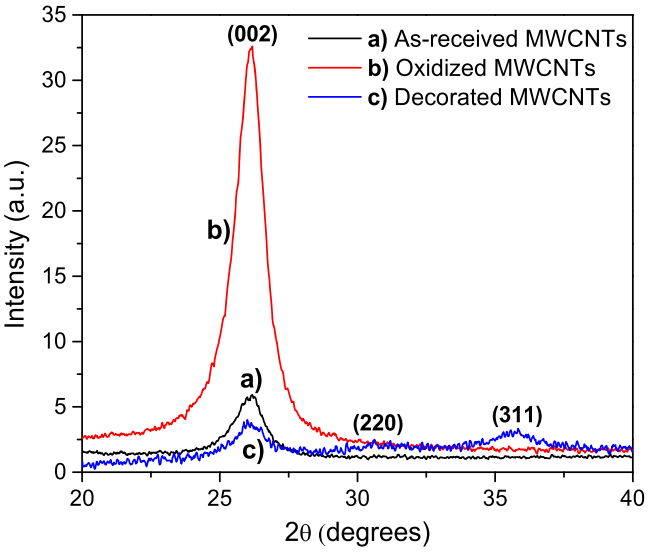

Figure 5. XRD patterns of (a) As-received MWCNTs (black line), (b) Oxidized MWCNTs (red line) and (c) Decorated MWCNTs with iron oxide nanoparticles (blue line).

groups in the MWCNTs walls, but at the same time, eliminates surface traces of amorphous carbon and metal impurities, these is the reason on the decrease in the value of I_G/I_D from as-received to oxidized samples.

On the other hand, the presence of two additional bands in the Raman spectra was observed, one at 122.29 cm^{-1}, which is attributed to the radial breathing mode (RBM) that is characteristic of single-wall carbon nanotubes (SWCNTs).[24] RBM corresponds to movements of the carbon atoms in the radial direction, as if the atom was breathing, this band appears between 120 and 350 cm^{-1} for MWCNTS with very few walls. In the case of the band observed at 2699.3 cm^{-1} for the oxidized MWCNTs and at 2700.6 cm^{-1} for as-received, they correspond to the overtone of the sp^2 hybridization disorders of carbon atoms generated by the amorphous material, and also with the other bands a shift with oxidation and decoration are observed.

In Raman spectra of decorated MWCNTs were observed different displacements of the main D (1355.00 cm^{-1}) and G (1584.09 cm^{-1}) bands compare with as-received and oxidized MWCNTs. In general, D, G, the overtone due to sp^2 hybridization and RBM bands, presented variations in their intensity and position.

Figure 5 presents the diffraction patterns of as-received, oxidized and decorated MWCNTs. The samples show a diffraction peak at angle $2\theta = 26.1°$ which is attributed to the (002) plane of MWCNTs.[25] This diffraction peak increases its intensity with de oxidation process (see the red line in Fig. 5), evidence of elimination of metal impurities and amorphous carbon; however decrease after the decoration process, for the presence of iron oxide nanoparticles. In the decorated MWCNTs, new 2θ diffraction angles indicate the presence of iron oxide nanoparticles.[26] Decorated MWCNTs exhibit new diffraction peaks at $2\theta = 30.6°$, 35.5° which correspond to the (220) and (311) planes of magnetite face-centered cubic (Fe_3O_4) but also overlap with maghemite (c-Fe_2O_3), according to the joint committee on powder diffraction standard (JCPDS) cards No. 19-629 for magnetite (Fe_3O_4) and No. 39-1346 for maghemite (c-Fe_2O_3).

Figure 6 shows thermogravimetric analysis under synthetic air flow of as-received, oxidized and decorated MWCNTs. The weight losses before approximately 150 °C is associated to evaporation of physio-sorbed water and possible decomposition of a few oxygen-containing groups. Decarboxylation and dehydration of functional groups it is expected that occur between 150 °C–350 °C for MWCNTs without decoration.[27] However, for decorated MWCNTs, the iron oxide

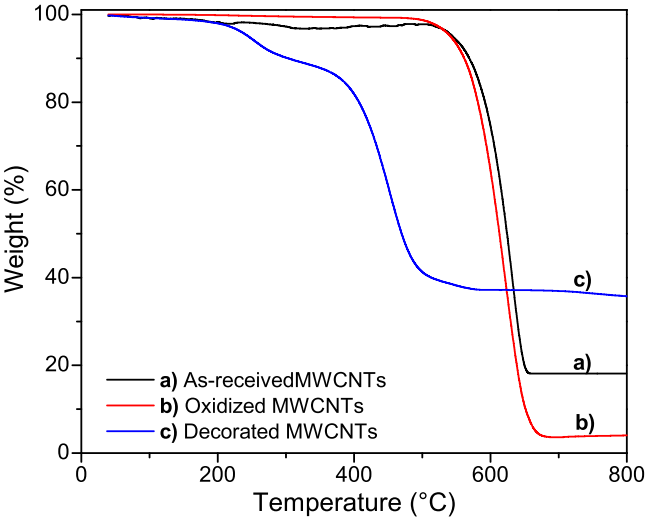

Figure 6. TGA of (a) As-received MWCNTs (black line), (b) Oxidized MWCNTs (red line) and (c) Decorated MWCNTs with iron oxide nanoparticles (blue line).

nanoparticles catalyze the thermal degradation of both amorphous carbon and the carbon nanostructure itself[20,27] producing a marked weight loss in the 200 °C–300 °C region. After this zone, thermal degradation of the graphitic structure (sp^2) of the MWCNTs occurs, which also occurs at lower temperatures for decorated samples.

The remaining weight of as-received and decorated MWCNTs after all the carbon material is burned off, provides valuable information about the amount of metallic impurities and iron oxide nanoparticles respectively. The as-received MWCNTs retained about 18 wt%, evidence of the metallic impurities present; after the oxidation process the MWCNTs only retained near of 4 wt% (evidence of the successful of this step) and finally the MWCNTs decorated with iron oxide nanoparticles retain 36 wt%, in agreement with the EDX results.

Figure 7 show XPS spectra of as-received MWCNTs (Fig. 7a), compared with oxidized and decorated MWCNTs after the laccase immobilization (Figs. 7b, 7c).

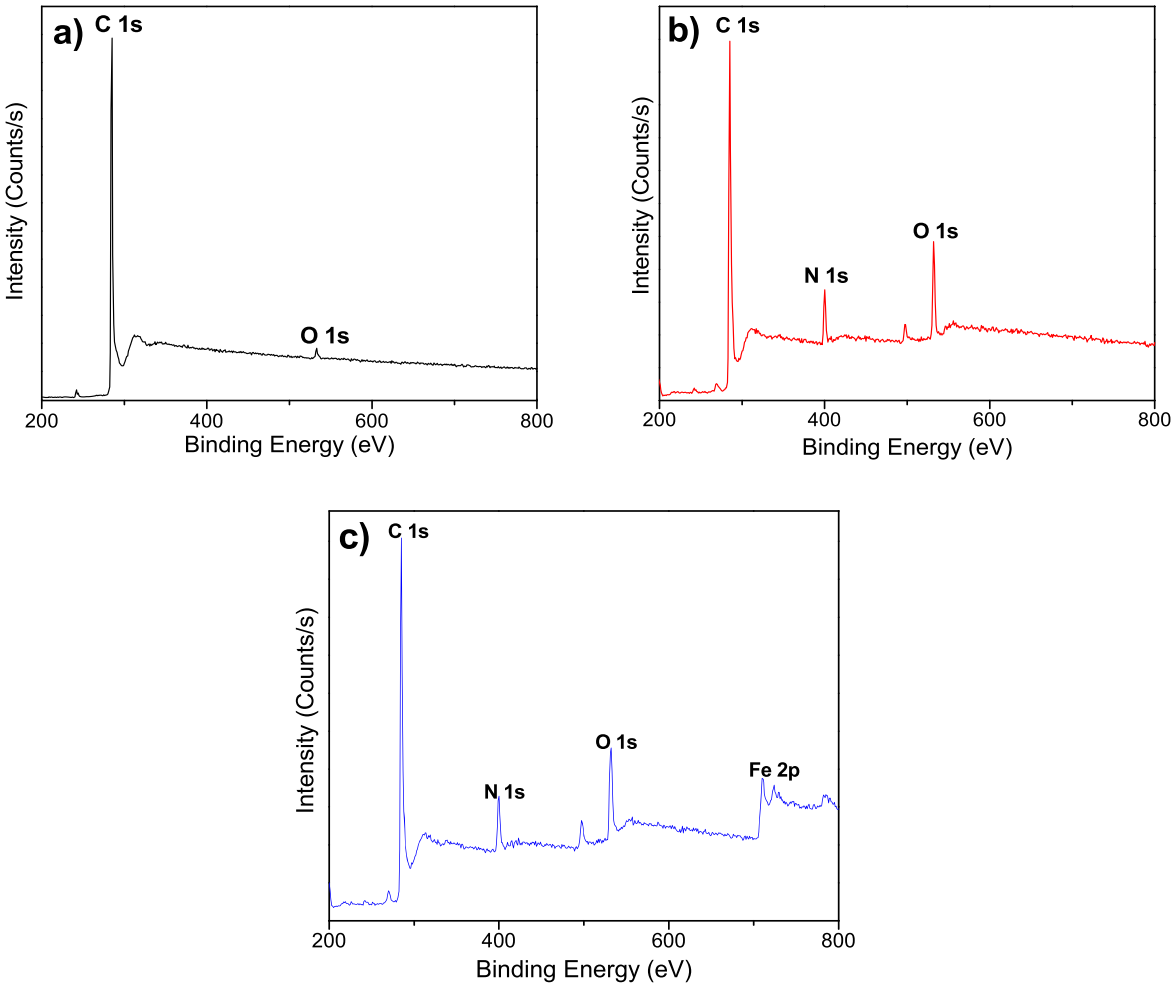

Figure 7. Survey of XPS spectrum of (a) As-received MWCNTs (before laccase immobilization), (b) Oxidized MWCNTs (after laccase immobilization) and (c) Decorated MWCNTs with iron oxide nanoparticles (after laccase immobilization).

Figure 7a shows the XPS survey of as-received MWCNTs (before laccase immobilization process) with bands at 285 and 532 eV which are attributed to the energetic distribution of C 1s and O 1s. Figure 7b shows the XPS survey of oxidized MWCNTs after the laccase immobilization process. This spectrum shows bands at 285, 400 and 532 eV which are attributed to the energetic distribution of C 1s, N 1s and O 1s respectively. The bands of C 1s and O 1s stayed with respect to the as-received samples, but the N 1s band appear. The N 1s band confirm the presence of laccase molecules in the sample. N 1s core levels of laccase layers deposited on MWNCT were originated from amino and imide groups for laccase deposited on oxidized (with carboxylic groups) MWCNTs and activated by EDAC and NHS.[27,28] The laccase enzyme used, was in solution, so that half the activity/number of units of enzyme immobilized via UV–vis result in 500 units ml^{-1}.

The XPS survey of decorated MWCNTs after the laccase immobilization (Fig. 7c) show bands at 285, 400, 532, and 711 eV which are attributed to the energetic distribution of C 1s, N 1s, O 1s, and Fe 2p respectively. The N 1s band is evidence of laccase immobilization originated from amino and imide groups deposited on decorated MWCNTs.[28,29] Fe $2p^{1/2}$ and Fe $2p^{3/2}$ bands located at 710 and 724 eV are related to Fe chemical states in Fe_3O_4;[20,30] and the orbital between Fe $2p^{1/2}$ and Fe $2p^{3/2}$ suggests that additional Fe states could be found in the c-Fe_2O_3 form.[31]

Electrochemical characterization.—The cyclic voltammetry characterization in a three electrodes system with and without sample as-received, oxidized and decorated MWCNTs were reported in a previous work,[18] emphasizing differences in behaviors for each type of MWCNTs and their redox peaks founded before enzymes immobilization. Herein, we will take the information obtained with the MWCNTs before the enzymatic immobilization in order to compare with the observed behavior in the same samples with the immobilized laccase enzyme, that is, the response of our bioelectrode Lac/MWCNTs/GCE and Lac/Fe_3O_4/MWCNTs/GCE when they are evaluated as an amperometric guaiacol biosensors.

Amperometric guaiacol sensing.—The objective of this work was to detect very small quantities of guaiacol (<0.1 μM), something new in this type of devices, with mainly interest in food industry, environmental and clinical analysis. In previous works, the detection of guaiacol starts 0.1 μM of concentration,[32,33] but there are no works that evaluate the range anticipated to 0.1 μM, which was evaluated in this work, whose idea is the detection of guaiacol free substances.

CV technique was used to evaluate the electrochemical biosensing properties (charge transfer) and the catalytic activity of laccase on the surface of GCE modified with MWCNTs, CV was evaluated using ABS solution (pH = 5.1) as electrolyte with different concentrations of guaiacol in a potential range between −0.7 to 0.7 V. This potential interval was used in many others works for laccase biosensors at the same operation conditions with different analytes and scan rates.[4,7,32–38]

Representatives cyclic voltammograms of GCE modified with oxidized and decorated MWCNTs containing immobilized laccase at 25 mV s^{-1} is shown in Fig. 8. Figure 8a show the comparative CV

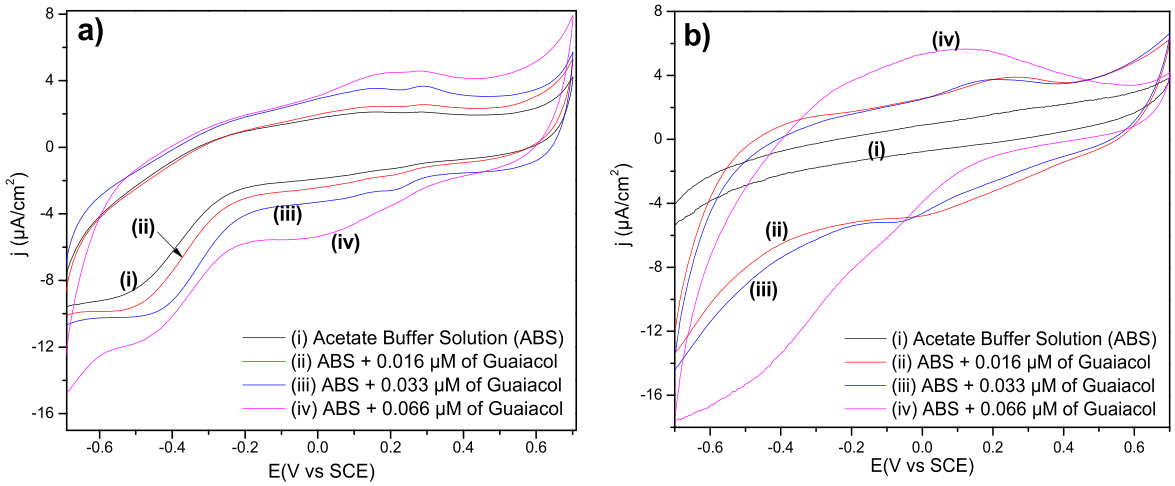

Figure 8. Cyclic voltammograms of MWCNTs containing laccase immobilized for increased guaiacol concentration in ABS. (a) Oxidized, (b) Decorated with iron oxide nanoparticles.

response of modified GCE with oxidized MWCNTs and laccase; voltammograms corresponding to each one at different electrolyte solutions. For ABS solution, the voltammogram is marked with number "i", and the voltammograms for ABS solution with three different concentrations of guaiacol added are marked with increasing roman numbers "ii," "iii" and "iv," corresponding to 0.016 μM; 0.033 μM and 0.066 μM of guaiacol respectively. It was observed that with the addition of small molar concentrations of guaiacol, the oxidation current was increased and the reduction current was decreased, that's reveal the improve of catalytic properties of the modified GCE. A well-defined quasi-reversible redox peak (~0.2 V vs SCE) was observed, evidence of the direct electron transfer between the laccase enzyme and the guaiacol in solution, that suggest the oxidation of guaiacol. The second cathodic peak observed at −0.4 V is related with the oxidation of functional groups in MWCNTs.[39]

The Fig. 8b shows the CV results of MWCNTs oxidized and decorated with iron oxide nanoparticles with laccase immobilized, the identification of voltammograms is similar to the Fig. 8a; ABS solution is marked with "i", and ABS solution with the three different concentrations of guaiacol are marked with increasing roman numbers "ii," "iii" and "iv," corresponding to 0.016 μM; 0.033 μM and 0.066 μM respectively. The representative voltammograms shows a similar CV behavior when add at ABS solution small concentrations of guaiacol, however, for the CGE with MWCNTs decorated with iron oxide nanoparticles and immobilized laccase (Fig. 8b), the changes in the oxidation and reduction currents are more notorious than the CGE with MWCNTs oxidized and immobilized laccase (Fig. 8a) with respect to free guaiacol solution; although the redox peaks are not symmetrical, the oxidation peak occurs at similar potential that the only oxidized samples (~0.2 V vs SCE), but the reduction peak moves to more negative potentials (~−0.05 V vs SCE), evidence of the presence of iron oxide nanoparticles.[33]

Oxidized MWCNTs with immobilized laccase enzyme (Fig. 8a) and decorated MWCNTs, same with laccase (Fig. 8b) show an oxidation symmetric peak at ~0.2 V, characteristic of activity of laccase enzyme immobilized on MWCNTs and metallic nanoparticles, when used as a guaiacol biosensor.[4,7,32–38] This redox peak is related to the oxidation and reduction of laccases when catalyze hydrogen abstraction reactions from phenolic and related substrates resulting in corresponding phenoxy radicals, they content four copper ions classified in one T1 Cu ion and a T2/T3 cluster. It has been shown that the T1 site is the primary redox center accepting electrons from the electron donors, the fully oxidized laccase is transformed in fully reduced laccase via internal electron transfer from copper sites, depending of immobilization method, pH, scan rate and diameter of the nanoparticle where it is immobilized.[32,40,41]

In Fig. 8 is not clear to compare between two types of enzymatic amperometric guaiacol biosensors (Fig. 8a for oxidized MWCNTs and Fig. 8b for decorated MWCNTs), the changes in current density with the subsequent addition of guaiacol are very similar. To better capture this effect, Fig. 9 plots the normalized changes in the current density ($\Delta j/j_0$, where j_0 is the initial current, that is when only use ABS solution as an electrolyte) directly proportional to guaiacol concentration for four replicates of the experiment showed in Fig. 8. The procedures were conducted for both currents, oxidation (Fig. 9a) and reduction (Fig. 9b). As seen from this figure, the changes in oxidation and reduction current densities are significantly higher when GCE is modified with MWCNTs decorated with iron oxide nanoparticles than when used MWCNTs only oxidized, clearly indicating the paramount role of the iron oxide nanoparticles in the electron transfer. A similar behavior was observed in previous work, for the development of amperometric glucose biosensors using MWCNTs, where emphasis the analysis of electrochemical behaviors before and after enzyme immobilization,[18] something that is not presented in this work.

By fitting a straight line to the data in Fig. 9 and using the area of the electrode, the amperometric sensitivity can be found and such a parameter is listed in Table II for both types of redox currents for each enzymatic amperometric biosensor. As well as observed changes in redox current densities, the slopes, the amperometric sensitivity values obtained are in concordance; higher values were observed in guaiacol biosensor prepared with decorated MWCNTs (71.202 and 110.186 μA mMcm^{-2} for oxidation and reduction current respectively), comparing with amperometric sensitivity values obtained with oxidized MWCNTs (64.919 and 63.487 μA mMcm^{-2} for oxidation and reduction current respectively). All amperometric sensitivities obtained were high compared to other amperometric laccase biosensors reported in the literature.[32]

Detection limits (DL) for the biosensors have been calculated using the following expression: DL = (3*SD)/S where SD is the standard deviation in peak oxidation current and S is the amperometric sensitivity of the electrode towards guaiacol. The detection limits of guaiacol are found to be about 9.227 nM and 7.238 mM for Lac/MWCNTs/GCE bioelectrodes configuration in oxidation and reduction current respectively, also 19.916 and 34.301 nM for bioelectrodes configuration Lac/Fe_3O_4/MWCNTs/GCE in oxidation and reduction current respectively; for the linear range 0–0.066 μM of guaiacol.

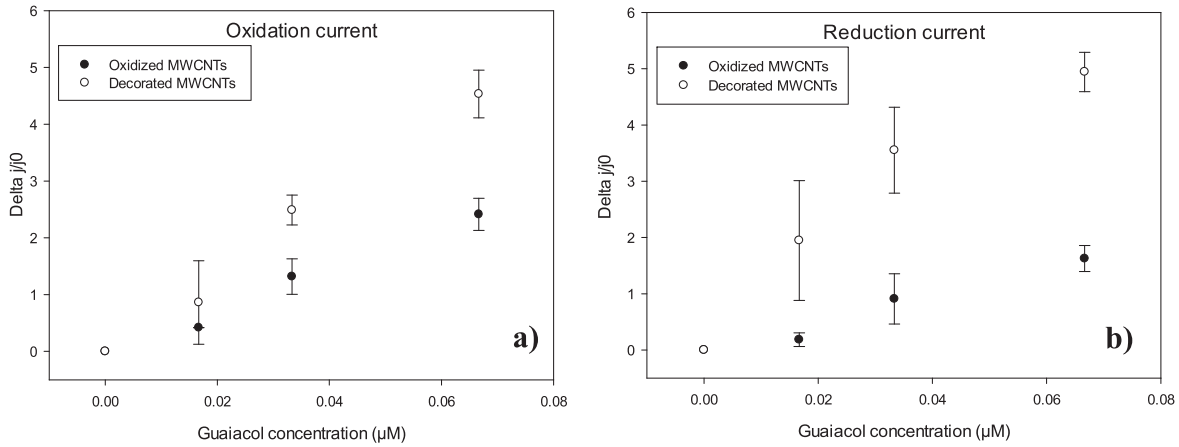

Figure 9. Normalized change in current density of oxidized and decorated MWCNTs upon increments in guaiacol concentration. (a) Oxidation current, (b) reduction current.

Table II. Amperometric sensitivity and detection limit obtained by CV.

MWCNTs treatment	Current type	Slope of linear adjustment (μM^{-1})	R^2	Amperometric sensitivity ($\mu A/\mu M\ cm^{-2}$)	Detection limit (nM)
Oxidation	Oxidation	37.381	0.988	64.919	9.227
	Reduction	25.716	0.969	63.487	7.238
Decoration	Oxidation	69.840	0.990	71.202	19.916
	Reduction	74.415	0.937	110.186	34.301

Conclusions

MWCNTs with immobilized laccase enzyme were used as a bioelectrode for electrochemical detection of small concentrations of guaiacol in ABS solutions. MWCNTs were subjected at two different treatments, first were oxidized by an acid treatment, generating a reactive surface with the incorporation of functional groups. Subsequent the oxidized MWCNTs were decorated with ~36% w/w iron oxide nanoparticles trough a solvothermal reaction. MWCNTs with different treatment (both, with laccase immobilized) were deposited in a GCE and tested in the amperometric detection of guaiacol.

The covalent immobilization of laccase enzyme over the MWCNTs was demonstrated by XPS analysis with the presence of N 1s band in immobilized samples, in the same way it was shown that the decoration with iron oxide nanoparticles does not blocked the enzyme immobilization.

Amperometric sensitivities of 64.919 and 63.487 μA mMcm^{-2} (for oxidation and reduction current respectively) was measured for the oxidized MWCNTs with laccase immobilized by cyclic voltammetry, while the decorated MWCNTs with laccase immobilized showed a sensitivities of 71.202 and 110.186 μA mMcm^{-2} (for oxidation and reduction current respectively). Detection limits were found 9.227 and 7.238 nM for Lac/MWCNTs/GCE, also 19.916 and 34.301 nM for Lac/Fe_3O_4/MWCNTs/GCE bioelectrodes configuration (in oxidation and reduction current respectively) in a linear range 0–0.066 μM of guaiacol.

Finally, it is concluded that the use of iron oxide nanoparticles decorating the MWCNT surface enhance the electron transfer, increasing the sensitivity and detection limit of guaiacol.

Acknowledgments

This research was supported by the project FIQI-2018-005 SEP-PRODEP (Mexico), responsible Uc-Cayetano in FIQ-UADY and Villanueva-Mena thanks for the fellowship for undergraduate student. The authors are grateful to project No. 268595 (CONACYT-Mexico) for the infrastructure for Raman spectroscopy. The technical assistance of A. May (CICY) and J.A. Chuc-Koyoc (FIQ-UADY) is strongly appreciated.

ORCID

E. G. Uc-Cayetano https://orcid.org/0000-0001-6002-6614

References

1. S. A. S. S. Gomes and M. J. F. Rebelo, "A new laccase biosensor for polyphenols determination." *Sensors*, **3**, 166 (2003).
2. A. Romani, M. Minunni, N. Mulinacci, P. Pinelli, F. F. Vincieri, M. Del Carlo, and M. Mascini, "Comparison among differential pulse voltammetry, amperometric biosensor, and HPLC/DAD analysis for polyphenol determination." *J. Agric. Food Chem.*, **48**, 1197 (2000).
3. M. Filipiak, "Electrochemical analysis of polyphenolic compounds." *Anal. Sci.*, **17**, 1667 (2001).
4. S. Chawla, R. Rawal, S. Sharma, and C. S. Pundir, "An amperometric biosensor based on laccase immobilized onto nickel nanoparticles/carboxylated multiwalled carbon nanotubes/polyaniline modified gold electrode for determination of phenolic content in fruit juices." *Biochem. Eng. J.*, **68**, 76 (2012).
5. R. Rawal, S. Chawla, and C. S. Pundir, "Polyphenol biosensor based on laccase immobilized onto silver nanoparticles/multiwalled carbon nanotube/polyaniline gold electrode." *Anal. Biochem.*, **419**, 196 (2011).
6. S. Gupta, C. N. Murthy, and C. R. Prabha, "Recent advances in carbon nanotube based electrochemical biosensors." *Int. J. Biol. Macromol.*, **108**, 687 (2018).
7. S. Chawla, R. Rawal, D. Kumar, and C. S. Pundir, "Amperometric determination of total phenolic content in wine by laccase immobilized onto silver nanoparticles/zinc oxide nanoparticles modified gold electrode." *Anal. Biochem.*, **430**, 16 (2012).
8. S. Rodríguez Couto and J. L. Toca Herrera, "Industrial and biotechnological applications of laccases: a review." *Biotechnol. Adv.*, **24**, 500 (2006).
9. S. Iijima, "Helical microtubules of graphitic carbon, Helical microtubules of graphitic carbon." *Nature*, **354**, 56 (1991).
10. M. F. L. De Volder, S. H. Tawfick, R. H. Baughman, and A. J. Hart, "Carbon nanotubes: present and future commercial applications." *Science*, **339**, 535 (2013).
11. L. Xiang, Y. Lin, P. Yu, L. Su, and L. Mao, "Laccase-catalyzed oxidation and intramolecular cyclization of dopamine: a new method for selective determination of dopamine with laccase/carbon nanotube-based electrochemical biosensors." *Electrochim. Acta*, **52**, 4144 (2007).
12. S. Dong, S. Zhang, L. Chi, P. He, Q. Wang, and Y. Fang, "Electrochemical behaviors of amino acids at multiwall carbon nanotubes and Cu_2O modified carbon paste electrode." *Anal. Biochem.*, **381**, 199 (2008).
13. H. M. So, D. W. Park, E. K. Jeon, Y. H. Kim, B. S. Kim, C. K. Lee, S. Y. Choi, S. C. Kim, H. Chang, and J. O. Lee, "Detection and titer estimation of *Escherichia coli* using aptamer-functionalized single-walled carbon-nanotube field-effect transistors." *Small*, **4**, 197 (2008).

14. H. Karimi-Maleh, F. Tahernejad-Javazmi, N. Atar, M. L. Yola, V. K. Gupta, and A. A. Ensafi, "A Novel DNA biosensor based on a pencil graphite electrode modified with polypyrrole/functionalized multiwalled carbon nanotubes for determination of 6-mercaptopurine anticancer drug." *Ind. Eng. Chem. Res.*, **54**, 3634 (2015).
15. V. Datsyuk, M. Kalyva, K. Papagelis, J. Parthenios, D. Tasis, A. Siokou, I. Kallitsis, and C. Galiotis, "Chemical oxidation of multiwalled carbon nanotubes." *Carbon*, **46**, 833 (2008).
16. L. C. Almeida, R. D. Correia, G. Squillaci, A. Morana, F. La Cara, J. P. Correia, and A. S. Viana, "Electrochemical deposition of bio-inspired laccase-polydopamine films for phenolic sensors." *Electrochim. Acta*, **319**, 462 (2019).
17. M. Dagys, P. Lamberg, S. Shleev, G. Niaura, I. Bachmatova, L. Marcinkeviciene, R. Meskys, J. Kulys, T. Arnebrant, and T. Ruzgas, "Comparison of bioelectrocatalysis at Trichaptum abietinum and Trametes hirsuta laccase modified electrodes." *Electrochim. Acta*, **130**, 141 (2014).
18. E. G. Uc-Cayetano, L. C. Ordóñez, J. V. Cauich-Rodríguez, and F. Avilés, "Enhancement of electrochemical glucose sensing by using multiwall carbon nanotubes decorated with iron oxide nanoparticles." *Int. J. Electrochem. Sci.*, **11**, 6356 (2016).
19. F. Avilés, J. V. Cauich-Rodríguez, L. Moo-Tah, A. May-Pat, and R. Vargas-Coronado, "Evaluation of mild acid oxidation treatments for MWCNT functionalization." *Carbon*, **47**, 2970 (2009).
20. E. G. Uc-Cayetano, F. Avilés, J. V. Cauich-Rodríguez, R. Schönfelder, A. Bachmatiuk, M. H. Rümmeli, F. Rubio, M. P. Gutierrez-Amador, and G. J. Cruz, "Influence of nanotube physicochemical properties on the decoration of multiwall carbon nanotubes with magnetic particles." *J. Nanopart. Res.*, **16**, 2192 (2014).
21. M. S. Dresselhaus, A. Jorio, A. G. Souza Filho, and R. Saito, "Defect characterization in graphene and carbon." *Phil. Trans. R. Soc. A*, **368**, 5355 (2010).
22. M. S. Dresselhaus, G. Dresselhaus, R. Saito, and A. Jorio, "Raman spectroscopy of carbon nanotubes." *Phys. Rep.*, **409**, 47 (2005).
23. E. F. Antunes, A. O. Lobo, E. J. Corat, V. J. Trava-Airoldi, A. A. Martin, and C. Veríssimo, "Comparative study of first- and second-order Raman spectra of MWCNT at visible and infrared laser excitation." *Carbon*, **44**, 2202 (2006).
24. A. Jorio, M. A. Pimenta, A. G. Souza Filho, R. Saito, G. Dresselhaus, and M. S. Dresselhaus, "Characterizing carbon nanotube samples with resonance Raman scattering." *New J. Phys.*, **5**, 139 (2003).
25. D. Zhang, L. Shi, J. Fang, and K. Dai, "Preparation and modification of carbon nanotubes." *Mater. Lett.*, **59**, 4044 (2005).
26. W. Jiang, K. L. Lai, H. Hu, X. B. Zeng, F. Lan, K. X. Liu, Y. Wu, and Z. W. Gu, "The effect of $[Fe^{3+}]/[Fe^{2+}]$ molar ratio and iron salts concentration on the properties of superparamagnetic iron oxide nanoparticles in the water/ethanol/toluene system." *J. Nanopart. Res.*, **13**, 5135 (2011).
27. K. A. Wepasnick, B. A. Smith, K. E. Schrote, H. K. Wilson, S. R. Diegelmann, and D. H. Fairbrother, "Surface and structural characterization of multi-walled carbon nanotubes following different oxidative treatments." *Carbon*, **49**, 24 (2011).
28. S. Malinowski, J. Jaroszynska-Wolinska, and P. A. F. Herbert, "Theoretical insight into plasma deposition of laccase bio-coating formation." *J. Mater. Sci.*, **54**, 10746 (2019).
29. M. Fernández-Fernández, M. Á. Sanromán, and D. Moldes, "Recent developments and applications of immobilized laccase." *Biotechnol. Adv.*, **31**, 1808 (2013).
30. T. Missana, C. Maffiotte, and M. García-Gutiérrez, "Surface reactions kinetics between nanocrystalline magnetite and uranyl." *J. Colloid. Interf. Sci.*, **261**, 154 (2003).
31. D. R. Kauffman, D. C. Sorescu, D. P. Schofield, B. L. Allen, K. D. Jordan, and A. Star, "Understanding the sensor response of metal decorated carbon nanotubes." *Nano Lett.*, **10**, 958 (2010).
32. M. M. Rodríguez-Delgado, G. S. Alemán-Nava, J. M. Rodríguez-Delgado, G. Dieck-Assad, S. O. Martínez-Chapa, D. Barceló, and R. Parra, "Laccase-based biosensors for detection of phenolic compounds." *Trends Anal. Chem.*, **74**, 21 (2015).
33. R. Rawal, S. Chawla, and C. S. Pundir, "An amperometric biosensor based on laccase immobilized onto Fe_3O_4NPs/cMWCNT/PANI/Au electrode for determination of phenolic content in tea leaves extract." *Enzyme Microb. Tech.*, **51**, 179 (2012).
34. C. Fernández-Sánchez, T. Tzanov, G. M. Gübitz, and A. Cavaco-Paulo, "Voltammetric monitoring of laccase-catalysed mediated reactions." *Bioelectrochemistry*, **58**, 149 (2002).
35. A. Swietlikowska, M. Gniadek, and B. Pałys, "Electrodeposited graphene nanostacks for biosensor applications. Surface groups as redox mediators for laccase." *Electrochim. Acta*, **98**, 75 (2013).
36. A. M. Nowicka, A. Kowalczyk, M. L. Donten, M. Donten, M. Bystrzejewski, and Z. Stojek, "Carbon-encapsulated iron nanoparticles as ferromagnetic matrix for oxygen reduction in absence and presence of immobilized laccase." *Electrochim. Acta*, **126**, 115 (2014).
37. R. S. Freire, N. Durán, and L. T. Kubota, "Effects of fungal laccase immobilization procedures for the development of a biosensor for phenol compounds." *Talanta*, **54**, 681 (2001).
38. K. Stolarczyk, E. Nazaruk, J. Rogalski, and R. Bilewicz, "Nanostructured carbon electrodes for laccase-catalyzed oxygen reduction without added mediators." *Electrochim. Acta*, **53**, 3983 (2008).
39. K. Kinoshita, *Carbon: Electrochemical and Physicochemical Properties* (John Wiley & Sons, New York) (1998).
40. F. Hollman and I. W. C. E. Arends, "Enzyme initiated radical polymerizations." *Polymers*, **4**, 759 (2012).
41. Z. Han, L. Zhao, P. Yu, J. Chen, F. Wu, and L. Mao, "Comparative investigation of small laccase immobilized on carbon nanomaterials for direct bioelectrocatalysis of oxygen reduction." *Electrochem. Commun.*, **101**, 82 (2019).
42. S. K. Vashist, D. Zheng, K. Al-Rubeaan, J. H. T. Luong, and F. S. Sheu, "Advances in carbon nanotube based electrochemical sensors for bioanalytical applications." *Biotechnol. Adv.*, **29**, 169 (2011).